THE JOURNAL OF BIOLOGICAL CHEMISTRY VOL. 290, NO. 31, pp. 19233–19244, July 31, 2015

Absence of the Regulator of G-protein Signaling, RGS4, Predisposes to Atrial Fibrillation and Is Associated with Abnormal Calcium Handling*

Received for publication, May 20, 2015, and in revised form, June 15, 2015 Published, JBC Papers in Press, June 18, 2015, DOI 10.1074/jbc.M115.666719

Aaisha Opel[‡§1], Muriel Nobles[§1], David Montaigne[§], Malcolm Finlay[§], Naomi Anderson[§], Ross Breckenridge[‡], and Andrew Tinker[‡§2]

From the [‡]British Heart Foundation Laboratories, Department of Medicine, University College London, Rayne Institute, London WC1E 6JJ, United Kingdom and the [§]William Harvey Heart Centre, Barts & The London School of Medicine & Dentistry, London EC1M 6BQ, United Kingdom

Background: Atrial fibrillation (AF) is the commonest arrhythmia. We understand little the factors that initiate AF.
Results: Loss of RGS4 promotes abnormal calcium release and is associated with AF.
Conclusion: Abnormal Ca^{2+} handling is important in the genesis of AF, and RGS4 is a potential new molecular participant.
Significance: Direct modulation of RGS4 may be an appropriate therapeutic approach.

The description of potential molecular substrates for predisposition to atrial fibrillation (AF) is incomplete, and it is unknown what role regulators of G-protein signaling might play. We address whether the attenuation of RGS4 function may promote AF and the mechanism through which this occurs. For this purpose, we studied a mouse with global genetic deletion of RGS4 ($RGS4^{-/-}$) and the normal littermate controls ($RGS4^{+/+}$). *In vivo* electrophysiology using atrial burst pacing revealed that mice with global RGS4 deletion developed AF more frequently than control littermates. Isolated atrial cells from $RGS4^{-/-}$ mice show an increase in Ca^{2+} spark frequency under basal conditions and after the addition of endothelin-1 and abnormal spontaneous Ca^{2+} release events after field stimulation. Isolated left atria studied on a multielectrode array revealed modest changes in path length for re-entry but abnormal electrical events after a pacing train in $RGS4^{-/-}$ mice. RGS4 deletion results in a predisposition to atrial fibrillation from enhanced activity in the $G\alpha_{q/11}$-IP_3 pathway, resulting in abnormal Ca^{2+} release and corresponding electrical events.

Atrial fibrillation (AF)[3] is the most common cardiac arrhythmia and affects at least 10% of the octogenarian population (1). Classically, it has been suggested that AF arises because of an atrial ectopic focus, a single re-entry circuit, or multiple re-entrant circuits (2) and a more modern interpretation involves the concept of rotors and spiral waves (3, 4). Such a rotor is thought to be present at the pulmonary vein-left atrial junction, with spiral waves emanating into the atria, giving fibrillation. Catheter ablation producing anatomical block between the pulmonary veins and left atrium can terminate AF and supports this hypothesis (5). Once AF has commenced, electrical remodeling occurs, particularly the decreased density of the L-type Ca^{2+} channel, leading to decreased effective refractory period (6). This is further exacerbated by concomitant structural remodeling and fibrosis (7). Thus there is an argument that effort should be made to understand how AF is initiated because preventing this will subsequently prevent the remodeling.

Regulators of G-protein signaling (RGS) act to deactivate G-protein signaling; they interact with the α-subunit and accelerate the intrinsic GTPase activity (8). There have been a number of studies indicating a potential influence of RGSs in determining cardiac electrophysiological responses (9–13). In this study, we focus on RGS4, which is known to negatively regulate both inhibitory $G\alpha_{i/o}$ and $G\alpha_{q/11}$ signaling (14–16). We address whether the attenuation of RGS4 function might act as a substrate for the initiation of AF and the mechanism by which this occurs.

Experimental Procedures

Experimental Animals—Mice were housed in accordance with UK Home Office guidelines relating to animal welfare, and the work was conducted under Project License PPL 70/6732. The environment was pathogen free, the temperature was controlled at 19–23 °C with 12-h day/night light cycles, and there

* This work was supported by British Heart Foundation Grant FS/09/042/27860, Wellcome Trust Grant 081475/Z/06/Z, and funds from the National Institute for Health Research Barts Cardiovascular Biomedical Research Unit, the Fondation Coeur et Artères, and Institut Servier. The authors declare that they have no conflicts of interest with the contents of this article.

[1] These authors contributed equally to the study.

[2] To whom correspondence should be addressed: William Harvey Heart Centre, Barts & the London School of Medicine & Dentistry, Charterhouse Square, London EC1M 6BQ, UK. Tel.: 20-7882-5783; E-mail: a.tinker@qmul.ac.uk.

[3] The abbreviations used are: AF, atrial fibrillation; HRV, heart rate variability; RGS, regulator of G-protein signaling; SNRT, sinus node recovery time; WCL, Wenckebach cycle length; AVNERP, atrioventricular nodal effective refractory period; ERP, effective refractory period; AERP, atrial effective refractory period; APD, action potential duration; ET-1, endothelin-1; ECT, extra Ca^{2+} transients; IP_3, inositol 1,4,5-trisphosphate; GIRK, G-protein gated inwardly rectifying K^+ channel; 2-APB, 2-aminoethoxydiphenylborate; PFA, paraformaldehyde; MEA, multielectrode array; EP, electrophysiology; CCh, carbachol; PR interval, interval on the ECG measured from the beginning of the P wave to the beginning of the R wave on the ECG; QRS, duration of the QRS complex on the ECG; corrected QT interval, from the beginning of the Q wave to the end of the T wave on the ECG corrected for heart rate.

was unlimited access to rodent chow and water. Mice were studied under standardized conditions once they were 8–16 weeks of age. The RGS4 KO mice were obtained from The Jackson Laboratory (Bar Harbor, ME) as part of the National Institutes of Health Deltagen/Lexicon Knock-out Mouse Resource. These mice had a global deletion of RGS4, and to generate them, the IRES LacZ-Neo cassette had been inserted to delete 58 base pairs of coding sequence and the entire first intron. The line was backcrossed for at least three generations onto the C57 black background.

Genotyping—Genomic DNA was extracted from mouse tail tips. Genotyping of the RGS4 KO mice was performed using 0.6 μl of each of three primers: moIMR0003 5′-GGG-CCA-GCT-CAT-TCC-TCC-CAC-TCA-T-3′, oIMR4946 5′-GGA-CAT-GAA-ACA-TCG-GCT-GGG-GTT-C-3′, and oIMR4947 5′-CCA-TCT-TGA-CCC-AAA-TCT-GGC-TCA-G-3′ and 1.2 μl of thermopolymerase buffer, 0.96 μl of 25 mM dNTP, 0.96 μl of 25 mM $MgCl_2$, 0.06 μl of 5 units/μl *Taq* polymerase, 5.02 μl of molecular water, and 2 μl of DNA. The following PCR program was utilized: 94 °C for 3 min, 35 cycles at 94 °C for 30 s, 63.5 °C for 1 min, and 72 °C for 1 min and then 72 °C for 2 min with storage of samples at 10 °C. An $RGS4^{+/+}$ mouse was denoted by a band seen at 227 bp, an $RGS4^{-/-}$ at 441 bp, and an $RGS4^{+/-}$ mouse had a band at both 227 and 441 bp.

Conscious Ambulatory Telemetry—Mice aged at least 12 weeks or weighing 20–25 g were operated on. Mice were anesthetized with 1.5% isoflurane, entrained with 0.2 liters per min of oxygen. A midline laparotomy was performed, and the telemetry probe (TA10EA-F20, DSI) was inserted into the abdominal cavity, taking care not to compress bowel and organs. A 2-mm horizontal incision was made at the right anterior chest wall, just below the clavicle and a second at the position of the cardiac apex. Each lead was tunneled through a sheath from the abdominal cavity via a small incision made in the peritoneum, one to the right anterior chest wall position, and the other to the cardiac apical position, giving a lead II ECG configuration. After a 2-week recovery period, ECG data were recorded on commercially available software (Dataquest ART v3) and analyzed for heart rate, ECG parameters (PR, QRS, and corrected QT interval), heart rate variability (HRV), atrial ectopics, and arrhythmias. The average heart rate was calculated from 48 h of continuous recording. 30-min segments, every 6 h over a 48-h period were examined for atrial ectopics, AF, sinus arrest, and heart block, as were segments where there was an apparent increase or decrease in heart rate. 0.5 mg/kg carbachol was injected intraperitoneally, and the heart rate was measured for 30 min. The average heart rate postinjection was calculated, and this segment was analyzed for atrial ectopics, AF, sinus arrest, and heart block. ECG segments for HRV assessment were analyzed between 12 to 2 p.m., when vagal tone is highest. A 30-min segment (divided into 15 2-min epochs by the software) was analyzed by the HRV module. Manual inspection of raw ECG tracings allowed any noise and artifact to be eliminated and ensured that every R wave was detected. Consecutive R waves were mathematically analyzed in time and frequency domains. All analysis was performed on LabChart 7 (ADInstruments) software.

Atrial Cell Isolation—Mice were injected with heparin, and beating hearts were removed under pentobarbital (3 ml/kg) and ketamine (1 ml/kg) anesthesia. The left and right atria were excised in normal Tyrode solution containing 140 mM NaCl, 5.4 mM KCl, 1.8 mM $CaCl_2$, 1 mM $MgCl_2$, 5 mM Hepes-NaOH, and 5.5 mM D-glucose, pH 7.4. Strips of tissues were enzymatically digested in a low Ca^{2+} and low Mg^{2+} solution containing 140 mM NaCl, 5.4 mM KCl, 0.5 mM $MgCl_2$, 0.2 mM $CaCl_2$, 1.2 mM KH_2PO_4, 50 mM taurine, 5.5 mM D-glucose, 5 mM Hepes-NaOH, pH 6.9. Collagenase type II (224 units/ml; Worthington), elastase (1.9 units/ml; Worthington), protease (0.9 units/ml; Sigma-Aldrich), and BSA (1 mg/ml) were added. The digestion step was carried out for 20 min under gentle mechanical agitation at 37 °C. Tissue strips were then washed out and transferred into a modified Kraftbrühe medium containing 70 mM L-glutamic acid, 20 mM KCl, 80 mM KOH, 10 mM D-β-OH-butyric acid, 10 mM KH_2PO_4, 10 mM taurine, 1 mg/ml BSA, and 10 mM Hepes-KOH, pH 7.4. Single atrial myocytes were manually dissociated in KB solution by employing a flame-forged glass pipette. Finally, extracellular Ca^{2+} concentration was recovered up to 1.3 mM. A drop of cell suspension was seeded onto sterilized laminin-coated coverslips. After 30–45 min, MEM cell culture medium was added, and cells were stored at 37 °C until used in humidified 5% CO_2-95% air at 37 °C. All experiments were performed at room temperature.

Single-cell Electrophysiology—Recordings were made with an Axopatch 200B amplifier (Axon Instruments) using fire-polished pipettes with a resistance of 3–4 MΩ pulled from filamented borosilicated glass capillaries (Harvard Apparatus, 1.5-mm outer diameter × 1.17-mm inner diameter). Data were acquired and analyzed by using a Digidata 1322A interface (Axon Instruments) and pCLAMP software (version 10; Axon Instruments). Action potentials were recorded in the current clamp mode. Atrial myocytes were stimulated using a 5-ms current pulse. The resting membrane potential, the magnitude of the initial depolarization, and the action potential duration at which 50 and 90% repolarization occurred were measured (APD_{50} and APD_{90}, respectively). The cells were clamped at −60 mV in an extracellular solution containing 135 mM NaCl, 5.4 mM KCl, 2 mM $CaCl_2$, 1 mM $MgCl_2$, 0.33 mM NaH_2PO_4, 5 mM H-HEPES, 10 mM glucose (buffered to pH 7.4 with NaOH). The intracellular solution was 110 mM potassium gluconate, 20 mM KCl, 10 mM NaCl, 1 mM $MgCl_2$, 2 mM MgATP, 2 mM EGTA, 0.3 mM Na_2GTP (buffered to pH 7.2 with KOH). To construct restitution curves, a pacing train of four impulses separated by 200 ms (S1) was followed by a single stimulus (S2). The interval between S1 and S2 ranged from 1000 to 20 ms. Methods were adapted from published protocols and our own published studies (17, 18). The extracellular and intracellular solutions were the same as described above for action potential recordings.

In Vivo EP Protocols—Mice aged 8 weeks underwent electrophysiological studies that were performed under general anesthesia with 1.5% isoflurane. The mouse was secured supine on a heating mat, and an ECG was attached in a lead II configuration, which was displayed on LabChart version 7.0 software (ADInstruments). Insensible heat loss was avoided through the use of the heating mat and an insulating blanket. At the start of the study, an ECG was recorded for 2 min to allow assessment

of heart rate and ECG parameters (PR, QRS, and corrected QT interval). The EPR-800 electrophysiological catheter (ADInstruments) was inserted via the right internal jugular vein into the right atrium through a venotomy. Optimal catheter position was characterized by atrial (A) and ventricular (V) signals, the ability to capture myocardium in the desired chamber, and rapid oscillations of the catheter representing contraction. To pace the heart, a S88 Grass stimulator was used. EP testing could only occur once myocardial capture was confirmed. Once achieved, the voltage was decreased to threshold capture voltage and then set to twice this to ensure consistent capture. Initially EP parameters were measured and subsequently, AF induction was performed.

Sinus Node Recovery Time (SNRT)—Atrial pacing was delivered at a rate of 600 bpm (cycle length, 100 ms) for 15 s and then switched off. The SNRT was measured from the last paced P-wave to the first return intrinsic P-wave. An average SNRT was calculated from three measurements.

Wenckebach Cycle Length (WCL)—Atrial pacing was commenced at 600 bpm and increased incrementally. The WCL was where a P-wave was not followed by a QRS complex, after successive prolongation of the PR interval. The 2:1 WCL was where two P-waves were seen for every QRS complex.

Atrioventricular Nodal Effective Refractory Period (AVNERP)—The ERP is the longest coupling interval at which capture no longer occurs. The AVNERP was performed by delivering a train of eight extra beats (S1) at 600 bpm followed by the delivery of a ninth beat (S2) at shorter and shorter coupling intervals until atrial capture occurred but ventricular capture was lost. The atrial effective refractory period (AERP) was performed in a similar fashion, only this time, an S2 was delivered until there was loss of atrial capture. This proved difficult in the mouse for reasons discussed in the main text.

AF Induction—Atrial burst pacing was found to be the most consistent method for AF induction. This was performed at a rate of 600 bpm (100-ms coupling interval) for 25 s, after which the pacing was switched off. The rate was subsequently increased in 10-ms decrements, the minimum coupling interval being 10 ms. Carbachol (0.5 mg/kg, intraperitoneally) was injected to decrease heart rate by at least 20% before burst pacing was repeated. An episode of AF was defined as an irregularly irregular rhythm with a normal QRS complex and no discernible P waves lasing for greater than 1 s. The arrhythmia was reproducible when it occurred and had to be induced on more than one occasion under identical conditions.

Cardiac Histology—Mice were subjected to terminal anesthesia with 1.5% isoflurane, and the hearts were quickly removed through a midline sternotomy. The hearts were rinsed in paraformaldehyde (PFA) and transferred to a scintillation vial with 10 ml of 4% PFA. This solution was made from 4 g of PFA dissolved in 100 ml of PBS. The hearts were then left gently shaking overnight to ensure adequate fixing. Hearts were rinsed once in PFA and then serially dehydrated with 30-min washes in varying concentrations of ethanol (diluted with PBS); 25%, 50%, 75%, and then 100% ethanol, in which they were stored at 4 °C. These dehydrated specimens were sectioned for histology after clearing them with Histo-Clear and wax embedding them. The specimens were stained with hematoxylin and eosin to decipher tissue architecture and Masson's trichrome to ascertain whether there was any fibrosis.

Calcium Imaging—Single atrial cardiomyocytes were isolated as described above. 50 μl of DMSO was added to 50 μg of fluo-4 acetoxymethyl ester (Invitrogen/Molecular Probes). Myocytes were loaded for 20 min with 2–5 μl of DMSO/fluo-4 and 5 μl of 20% pluronic acid in 1 ml of recording buffer. Recording buffer contained 135 mM NaCl, 2.7 mM KCl, 2 mM $CaCl_2$, 1 mM $MgCl_2$, 0.33 mM NaH_2PO_4, 5 mM HEPES, 10 mM glucose, pH 7.4.

For the Measurement of Ca^{2+} Sparks—The cells were then rinsed with recording buffer before imaging with a confocal microscope (Zeiss Axiovert 200 M) in line scan mode (2.3 ms per scan; pixel size, 0.2 μm). The cells were excited using a 488-nm laser line, and emission was measured using a LP510 filter. Three lines were performed per cell (top, middle, and bottom) across its longitudinal axis. Following the acquisition of line scans, 1 mM caffeine (1,3,7-trimethyl xanthine) was added to the dish, and calcium release was recorded as a time series. In a separate set of studies, after the lines scans were performed, drugs were added. 100 nM endothelin-1 (ET-1) was added, and after a 2–4-min equilibration time, line scans were repeated. In separate experiments, 5 μm 2-aminoethoxydiphenylborate (2-APB) was added and allowed to equilibrate before the addition of 100 nM endothelin-1. Line scans were repeated as before. Analysis of the calcium sparks was made by Sparkmaster (19). Calcium sparks were quantified in terms of amplitude (F/F_0), full-width at half-maximum amplitude (μm), duration at half-maximum amplitude (ms), time to peak (ms), Tau (ms), and frequency of sparks. Calcium release following the administration of caffeine was expressed as a ratio [(max − background)/(min − background)].

For the Measurement of Ca^{2+} Transients in Field Stimulated Cells—Cells were imaged with a confocal microscope (Zen LSM 510) in line scan mode. Fluo-4 is excited by 488-nm argon laser, and emission was collected using a LP525 filter. Experiments were performed at 37 °C. One line was performed per cell across its transverse axis. Ca^{2+} transients are elicited by field stimulation through a pair of electrodes with a pulse delivered by a Grass S88 stimulator connected to a stimulus isolation unit. Cells were stimulated at 1 Hz (4V, 5 ms, bipolar pulse) for at least 2–3 min to reach a steady state before recording. Images are analyzed using ImageJ software. We identified extra Ca^{2+} transients (ECTs) as spontaneous Ca^{2+} increase that are at least 20% of a Ca^{2+} transient evoked by stimulation (see Fig. 6*A*).

For the Measurement of Ca^{2+} Transients in Atrial Tissue—Atrial tissue was dissected after a period of perfusion with cold oxygenated Krebs buffer on the Langendorff setup. The tissue was loaded with Fluo-4 and imaged on Nikon Eclipse TE200 inverted microscope with an integrated Digital CMOS camera (ORCA Flash4.0 V2 C11440–22CU; Hamamatsu Photonics UK Limited, Hertfordshire, UK). A light emitting diode illumination system was synchronized with the camera for epifluorescence.

Measurement of Atrial Electrophysiology Using Multielectrode Arrays—Left atria were dissected from isolated mouse hearts after mounting in a Langendorff setup and perfused with Krebs solution supplemented with 30 mM 2,3-butanedione

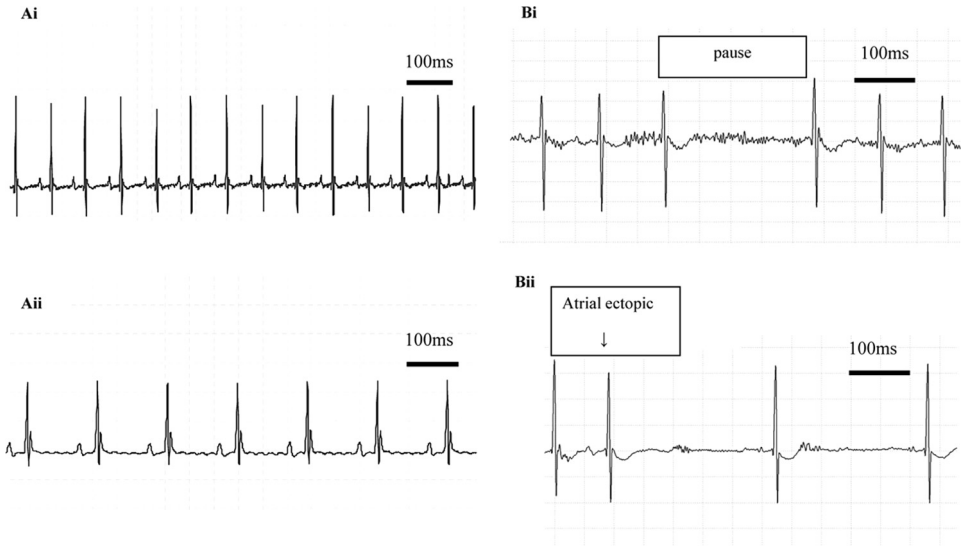

FIGURE 1. **Heart rhythm in awake mice studied using radiotelemetry.** *A*, resting ECG (*panel i*) and ECG showing bradycardia with carbachol (*panel ii*). *B*, atrial pause (*panel i*) and atrial ectopic (*panel ii*). After the administration of CCh, the RGS4$^{-/-}$ mice had several pauses and between two and seven atrial ectopics

TABLE 1

Telemetry results of RGS4$^{-/-}$ mice compared with RGS4$^{+/+}$ littermate controls

Normalized high-frequency power (nHF) and normalized low-frequency power (nLF) are normalized to exclude TP and are expressed in normalized power units. RMSSD, root mean square of successive differences; SDn-n, standard deviation of "normal" sinus R-R/n-n intervals; TP, total power; VLF, very low frequency (<0.4 Hz); LF, low frequency (0.4–1.5 Hz); HF, high frequency (1.5–4.0 Hz).

	Means ± S.E.			Means ± S.E.		*p* value		
	RGS4$^{+/+}$ (n = 6)	RGS4$^{-/-}$ (n = 5)	*p* value RGS4$^{+/+}$/RGS4$^{-/-}$	RGS4$^{+/+}$ with CCh (n = 6)	RGS4$^{-/-}$ with CCh (n = 5)	RGS4$^{+/+}$/RGS4$^{-/-}$ with CCh	RGS4$^{+/+}$/RGS4$^{+/+}$ with CCh	RGS4$^{-/-}$/RGS4$^{-/-}$ with CCh
Mean HR (bpm)	562.6 ± 36.3	634.3 ± 52.6	0.030	524.3 ± 24.2	288.2 ± 37.9	0.020	0.480	0.008
PR (ms)	35.1 ± 0.5	34.1 ± 0.7	0.330	33.6 ± 0.8	30.1 ± 6.0	0.790	0.130	1.000
QRS (ms)	9.0 ± 0.4	9.7 ± 0.6	0.660	9.7 ± 0.6	8.8 ± 0.4	0.660	0.700	0.310
QT_C (ms)	50.6 ± 2.7	57.2 ± 2.8	0.250	62.9 ± 7.1	30.6 ± 3.0	0.004	0.390	0.008
RMSSD (ms)	11.4 ± 0.9	11.2 ± 1.6	0.540	25.6 ± 6.1	40.2 ± 9.5	0.330	0.180	0.008
SDn-n (ms)	12.3 ± 0.4	11.1 ± 1.1	0.330	24.8 ± 4.3	54.6 ± 15.2	0.130	0.060	0.008
TP (ms^2)	126.6 ± 11.4	113.0 ± 20.0	0.660	689.7 ± 201.9	2431.1 ± 1452.3	0.430	0.060	0.008
VLF (ms^2)	25.0 ± 3.4	16.0 ± 4.6	0.250	93.1 ± 36.6	741.4 ± 529.1	0.130	0.390	0.008
LF (ms^2)	15.5 ± 2.0	11.9 ± 2.4	0.330	75.7 ± 31.2	433.3 ± 315.4	0.250	0.090	0.008
nLF (nu)	15.3 ± 1.0	12.1 ± 3.0	0.79	13.6 ± 5.1	19.6 ± 4.4	0.33	0.06	0.31
HF (ms^2)	18.7 ± 2.3	14.0 ± 3.5	0.43	78.8 ± 25.8	381.1 ± 254.6	0.43	0.06	0.008
nHF (nu)	19.0 ± 2.4	15.7 ± 4.5	0.43	14.8 ± 4.0	18.1 ± 4.0	0.93	0.24	0.69
LF/HF	0.9 ± 0.1	0.9 ± 0.1	0.93	0.8 ± 0.1	1.3 ± 0.4	0.33	0.48	0.84

monoxime. The tissue was then transferred to the array perfused with Krebs solution (37 °C; 95%O_2, 5%CO_2). Left atrial electrophysiology was assessed during electrical stimulation using a multielectrode array (MEA) system which allows non-invasive synchronous multifocal recording of extracellular field potentials (20). The MEA (MEA2100; Multi Channel Systems, Reutlingen, Germany) consists of 60 microelectrodes arranged in an 8 × 8 matrix, with a 20-μm electrode diameter and an interelectrode distance of 200 μm. Myocardial samples were positioned in the center of the MEA dish, held in contact with electrodes by a holder, and continuously superfused with oxygenated Krebs solution at 37 °C. Baseline electrical stimulation (bipolar pulses, 2× threshold, 2-ms duration, 4-Hz frequency) was applied via one of the MEA microelectrodes. Field potential data were acquired simultaneously from all 60 microelectrodes. S1-S2 train stimulation with a S1-S1 cycle length of 250 ms was used to assess AERP. Spontaneous electrical activity was also identified with the MEA system during S1-S2 stimulation protocols in the absence and the presence of 10 nM ET-1. To assess conduction properties, isolated atria were sequentially stimulated (4 Hz) from one electrode of each of the four edges of the array. Field potential recordings obtained in these conditions were processed using LabChart7 (ADInstrument) to define local activation time based on minimum of the derivative of field potential. Average conduction velocity was calculated by linear regression relating interelectrode distance to activation times, as previously described (21). The slope of the regression line was the average conduction velocity. Minimal wave front cycle length was calculated for each isolated atria as AERPxCV.

Statistical Analysis—The mean and standard error of the mean are presented. The nonparametric Mann-Whitney test was used to analyze ECG and EP parameters, calcium sparks, and AF duration, and the Fisher's exact test was used to analyze AF occurrence. A p value of <0.05 was statistically significant. Statistical analysis was performed using commercially available software, GraphPad Prism version 4.00 (GraphPad Software, San Diego, CA).

Results

Radiotelemetry in RGS4$^{-/-}$ Mice—RGS4$^{+/-}$ heterozygotes were bred together, and RGS4$^{-/-}$ offspring were studied together with RGS4$^{+/+}$ littermate controls. We first investi-

gated whether RGS4$^{-/-}$ had evidence of spontaneous atrial arrhythmia using radiotelemetry at 3 months of age. RGS4$^{-/-}$ mice were tachycardic when compared with RGS4$^{+/+}$ mice but had an enhanced bradycardic response to carbachol. ECG parameters in the two groups of conscious mice were comparable (Fig. 1*A* and Table 1) except that the corrected QT duration measured in RGS4$^{-/-}$ mice in the presence of CCh was shorter. Statistically, HRV parameters of RGS4$^{+/+}$ and RGS4$^{-/-}$ mice with and without CCh were comparable, although there was a trend to greater variation with CCh in the RGS4$^{-/-}$ mice (Table 1). 30 min resting ECG traces showed no atrial ectopics, AF, sinus arrest, or heart block in either group of mice. In contrast, after the administration of CCh the RGS4$^{-/-}$ mice had several pauses (Fig. 1*B*), between two and seven atrial ectopics (Fig. 1*B*), but no episodes of AF or heart block. At most, RGS4$^{+/+}$ littermate control mice had one atrial ectopic and no pauses.

TABLE 2
ECG and EP parameters measured during EP study
Comparisons of the ECG and EP parameters between RGS4$^{+/+}$ and RGS4$^{-/-}$ are not significant ($p > 0.05$).

	Means ± S.E.	
	RGS4$^{+/+}$	RGS4$^{-/-}$
ECG parameters[a]		
Heart rate (bpm)	521.2 ± 7.5	508.3 ± 10.2
PR (ms)	37.4 ± 0.1	36.7 ± 0.7
QRS (ms)	8.4 ± 0.1	8.4 ± 0.2
QT_C (ms)	55.6 ± 1.5	58.1 ± 3.4
EP parameters[b]		
SNRT (ms)	165.4 ± 14.3	167.0 ± 11.0
WCL (ms)	78.3 ± 2.4	79.2 ± 2.1
2:1 WCL (ms)	61.0 ± 1.8	61.4 ± 2.4
AVNERP (ms)	65.8 ± 6.0	56.1 ± 2.7

[a] $n = 56$ for RGS4$^{+/+}$, and $n = 16$ for RGS4$^{-/-}$.
[b] $n = 32$ for RGS4$^{+/+}$, and $n = 13$ for RGS4$^{-/-}$.

RGS4$^{-/-}$ Mice Have Inducible Atrial Fibrillation—In the absence of spontaneous arrhythmia, we proceeded to perform *in vivo* electrophysiology (EP) studies and programmed electrical stimulation in anesthetized unconscious mice. There were no significant differences in the ECG or EP parameters between

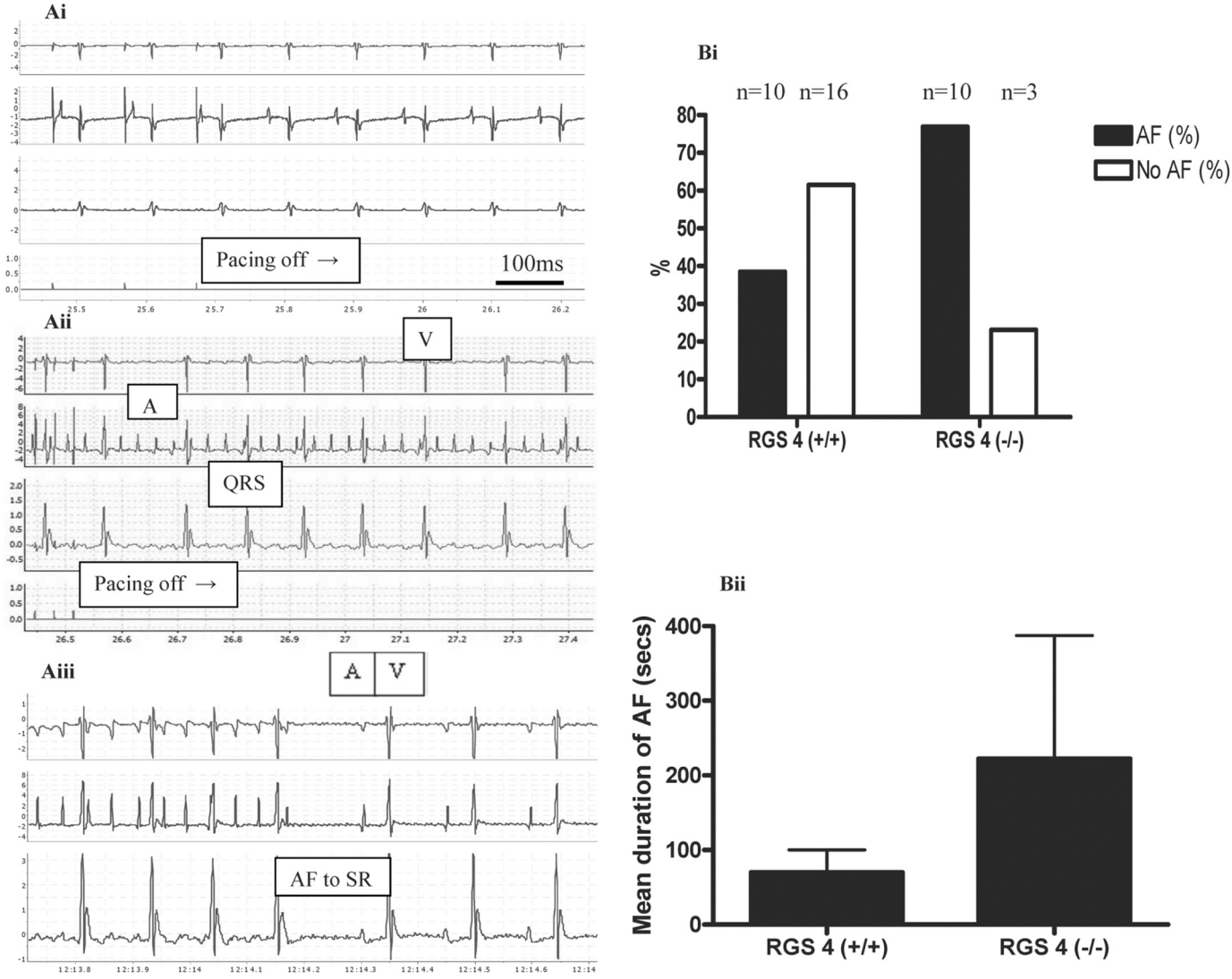

FIGURE 2. **Induction of AF using burst pacing.** *A*, no AF induced after 25 s of burst pacing in the RGS4$^{+/+}$ mouse. *Panel i*, sinus rhythm continues when pacing is switched off. *Panel ii*, AF diagnosed on the surface ECG and intracardiac electrograms following 25 s of atrial burst pacing in the RGS4$^{-/-}$ mouse. *Panel iii*, termination of AF to sinus rhythm. *B*, percentage of mice in whom AF was induced. *Panel i*, absolute numbers are shown above bar graphs. *Panel ii*, mean duration of AF. *A*, atrial electrogram; *V*, ventricular electrogram; *QRS*, QRS complex; *SR*, sinus rhythm.

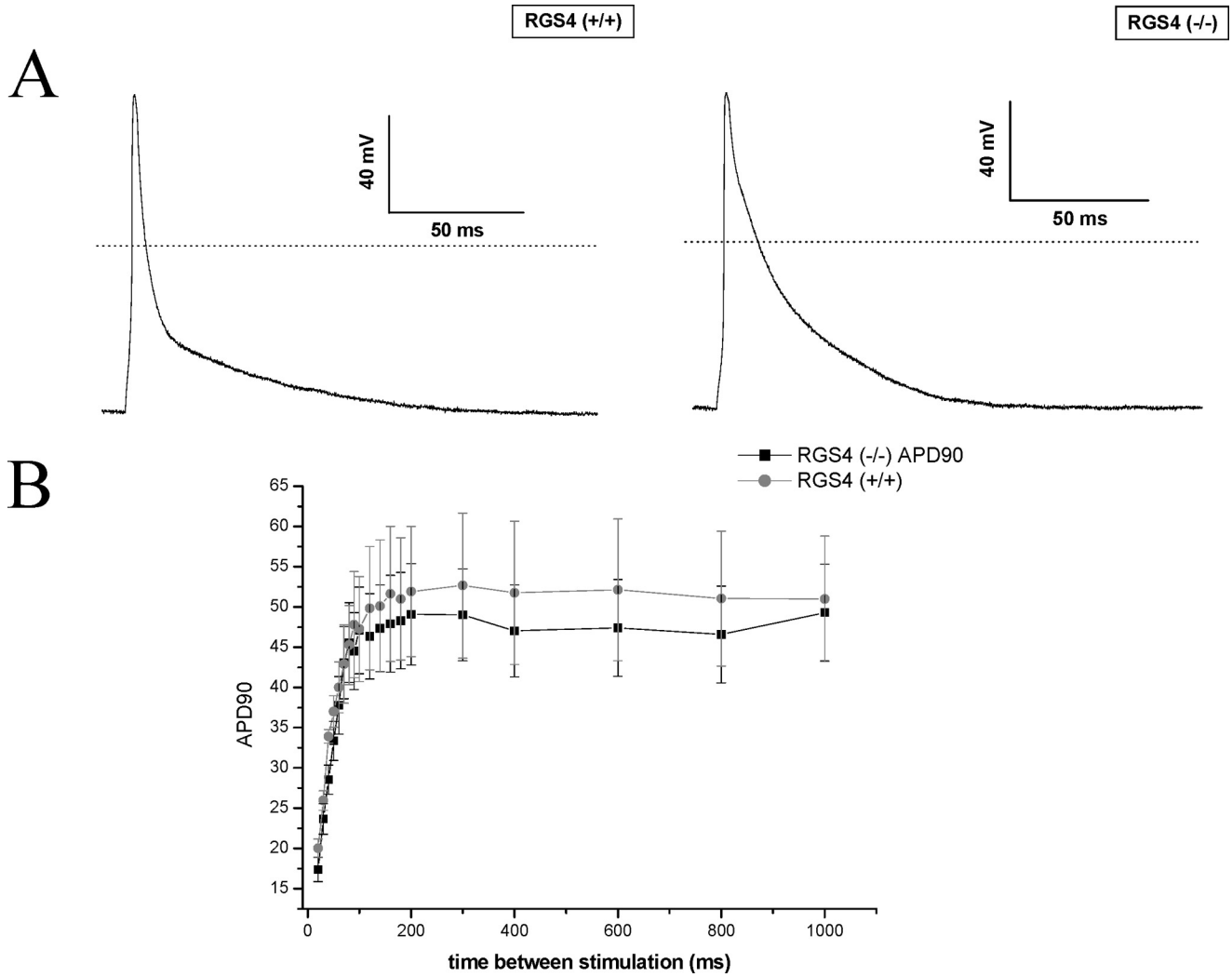

FIGURE 3. **The electrophysiology of single atrial cells.** *A*, atrial action potentials are shown for RGS4$^{+/+}$ and RGS4$^{-/-}$ mice. Representative traces of an action potential measured after stimulation of a cell by a 5-ms pulse after pacing at 1 Hz for 60 s. *B*, single-cell restitution that was not different between the two lines of mice.

TABLE 3
Mean action potential parameters
Em, resting membrane potential.

Parameter	RGS4$^{+/+}$ ($n = 15$)	RGS4$^{-/-}$ ($n = 12$)	*P*
Cell capacitance (pF)	41.6 ± 4.3	35.7 ± 3.6	0.31
Em (mV)	−69.1 ± 1.7	−67.2 ± 1.4	0.42
Δ (mV)	133.3 ± 11	124 ± 4	0.51
APD_{50} (ms)	10.4 ± 0.8	15.1 ± 2	0.03
APD_{90} (ms)	67 ± 6.3	64.5 ± 4.5	0.77
Total (ms)	126 ± 9.4	114 ± 9.3	0.38

control and RGS4$^{-/-}$ under these conditions (Table 2). However, when we used burst atrial pacing to induce AF, the RGS4$^{-/-}$ mice were more susceptible to AF; 10 of 13 RGS4$^{-/-}$ mice developed AF compared with 10 of 26 RGS4$^{+/+}$ ($p = 0.04$; Fig. 2). In addition there was a trend for the RGS4$^{-/-}$ mice to have a longer duration of AF, although this was not statistically significant (Fig. 2*B*). In some cases the supraventricular arrhythmia resembled atrial tachycardia or flutter, but the ventricular response was irregularly irregular, and it is referred to as AF below. Carbachol did not increase the likelihood of AF induction using burst pacing in RGS4$^{-/-}$ or control mice ($p = 0.28$). Measurement of the AERP was not achieved as the S2 was being delivered at a short coupling interval and abutted the QRS complex. Although during this time one would assume that atrial capture should not occur, the morphology of this QRS complex was sometimes different from other complexes, which may suggest that a P-wave was buried within it. The intracardiac electrograms were unhelpful, because one cannot pace and sense simultaneously from the same electrode , and the remaining sensing channels were sometimes removed from the chamber of interest to show clear intracardiac atrial electrograms. For these reasons, the AERP could not be reliably and consistently determined using this technique. However, we made single-cell and *ex vivo* tissue measurements to investigate ERP and further characterize the arrhythmic substrate (see below).

Single-cell Electrophysiology in RGS4$^{-/-}$ Mice—We studied the characteristics of the action potential duration (APD) by using patch clamping on freshly dissociated single atrial cells. The early phase of repolarization was significantly prolonged in RGS4$^{-/-}$ mice compared with control as reflected in a prolonged APD_{50} (Fig. 3*A* and Table 3). However, there were no significant

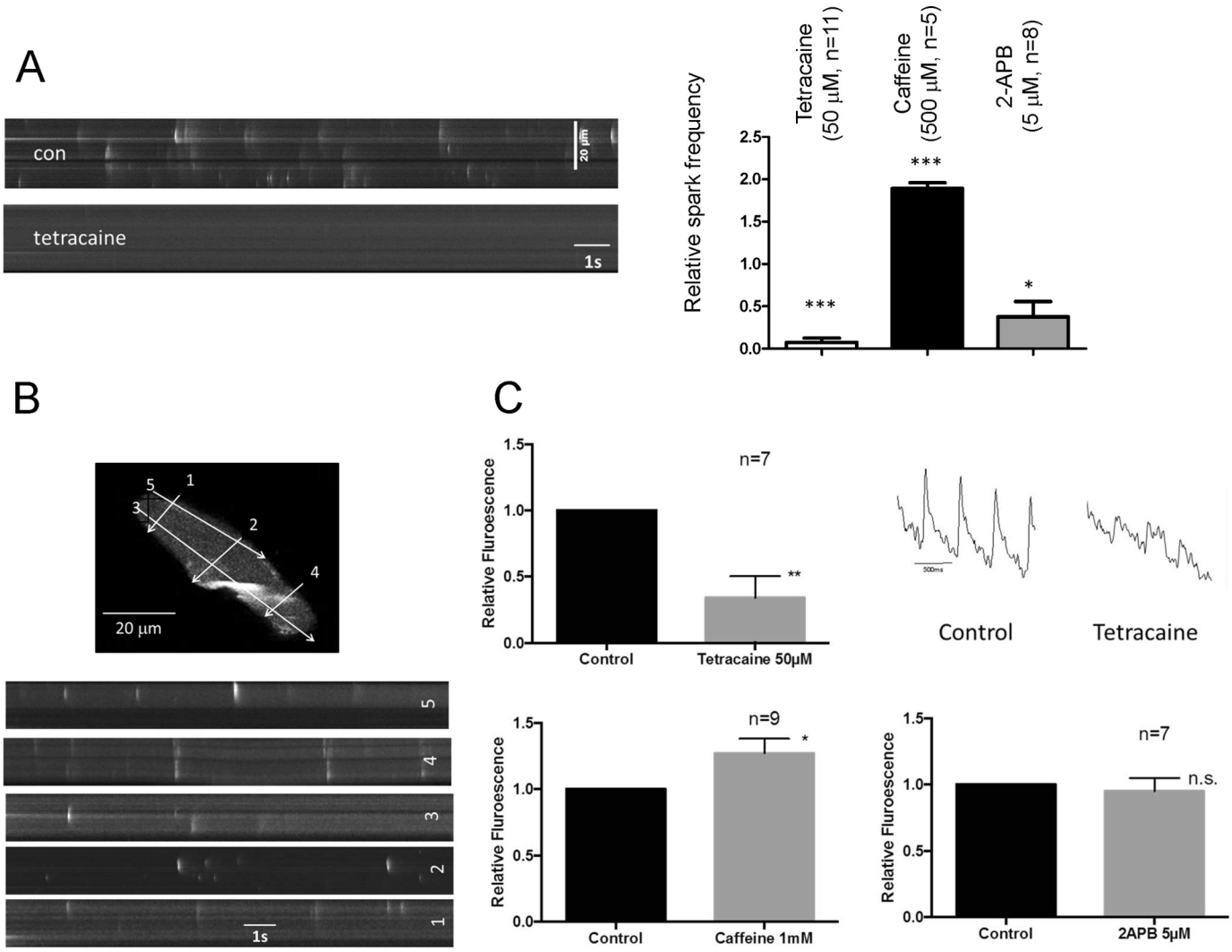

FIGURE 4. **Calcium handling in murine atria.** *A*, the effects of tetracaine, caffeine, and 2-APB on calcium sparks in single myocytes isolated from murine atria. *con*, control. *B*, the spatial location of the sparks from different line scans on a single myocyte. *C*, the effect of tetracaine, caffeine, and 2-APB on Ca^{2+} transients in intact atrial tissue.

differences were observed for other action potential parameters. There was no evidence for a shortened APD_{90} or APD that might lead to a decreased AERP (Table 1). We next examined the interval dependence of action potential shortening by constructing single cell restitution curves as previously described (17, 18). There were no significant differences between the $RGS4^{-/-}$ and $RGS4^{+/+}$ mice under basal conditions (Fig. 3*B*).

G-protein-gated inwardly rectifying K^+ (GIRK) channels are an excellent system for assessing the involvement of RGS proteins in GAP activity at inhibitory G-proteins (22). Cifelli *et al.* (9) established that RGS4 plays an important role in regulating sinus rhythm by inhibiting parasympathetic signaling and GIRK activity (9). The authors found that deletion of RGS4 led to alteration of GIRK kinetics in cardiomyocytes from the sinoatrial node with attenuation of rapid desensitization along with an increase in the time for signal deactivation following agonist withdrawal. They did not study atrial cells, and thus we studied the kinetics of GIRK currents in isolated atrial cardiomyocytes by using a 20-s application of carbachol at a holding potential of −60 mV. Currents showed a similar amplitude ($p > 0.05$ for both basal and agonist induced currents) in both $RGS4^{+/+}$ (basal = −92.7 ± 6.16, agonist induced = −101.4 ± 11.4 pA/pF, $n = 36$) and $RGS4^{-/-}$ atrial myocytes (basal = −78.2 ± 6.2, agonist induced = −83 ± 15 pA/pF, $n = 27$). There was also no change in the kinetics of activation measured as time to peak activation (usually occurring with an initial lag phase followed by an activation phase to peak current referred to as lag + time to peak (23)) from agonist application ($RGS4^{+/+}$ = 0.94 ± 0.04; $RGS4^{-/-}$ = 0.83 ± 0.04 s, $p > 0.05$) and neither in the degree of desensitization measured as a percentage decrease in agonist induced current from peak activation after 20 s of agonist application ($RGS4^{+/+}$ = 32.8 ± 2.7; $RGS4^{-/-}$ = 31 ± 2.5%, $p > 0.05$). The only significant difference was obtained for the time constant for deactivation of the GIRK current, with paradoxically a faster deactivation in the $RGS4^{-/-}$ myocytes 2.12 ± 0.21 s compared with $RGS4^{+/+}$ 3.54 ± 0.35s ($p = 0.02$). Thus, in atrial myocytes, in contrast to cells from the SA node, with RGS4 deletion, there is no evidence for a significant role of RGS4 in enhancing the intrinsic GTPase activity of inhibitory G-proteins.

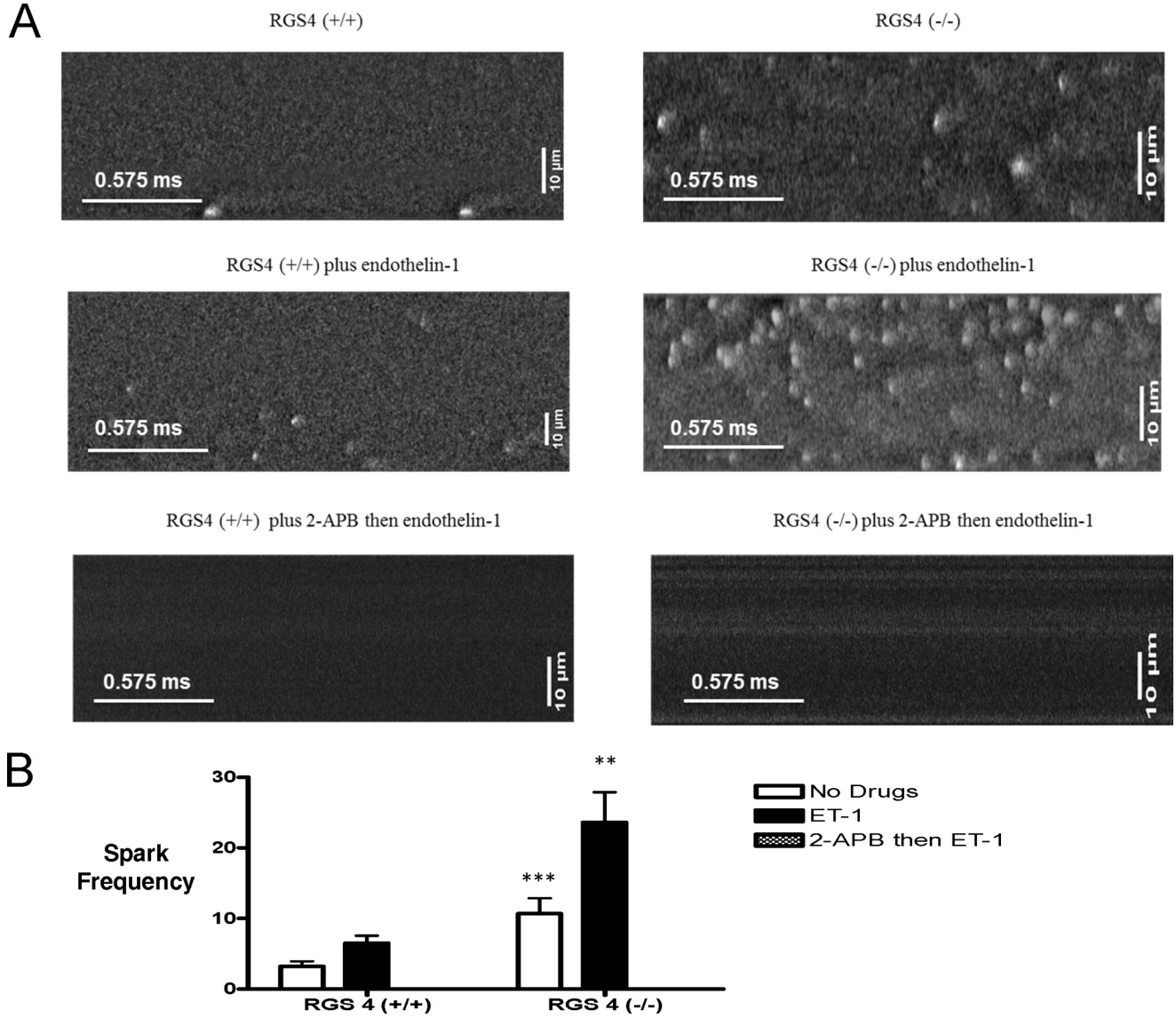

FIGURE 5. **The effect of RGS4 on elemental calcium release events.** *A*, line scan images of calcium sparks in RGS4$^{+/+}$ and RGS4$^{-/-}$ mice, alone, with ET-1 and 2-APB and then ET-1. Please note that these are different individual cells because only a subset of cells was studied before and after ET-1 administration. The frequency of sparks was (sparks/100 μm/s) greater in RGS4$^{-/-}$ mice compared with RGS4$^{+/+}$ and increased further with ET-1. No sparks were seen with 2-APB. The images shown in the figure have been filtered. The *bottom left scale bar* represents 0.575 ms, and the *top left scale bar* is 10 μm. *B*, calcium spark frequencies (of RGS4$^{+/+}$ and RGS4$^{-/-}$ mice, alone, with ET-1 and 2-APB and then ET-1. The frequency of sparks was greater in RGS4$^{-/-}$ mice compared with RGS4$^{+/+}$ and increased further with ET-1. **, $p < 0.01$; ***, $p < 0.001$. No sparks were seen with 2-APB.

TABLE 4

Calcium spark characteristics of RGS4$^{-/-}$ mice and RGS4$^{+/+}$ alone, with ET-1 and 2-APB then ET-1

Amplitude (F/F_0) full-width at half-maximum amplitude (FWHM, μm), duration at half-maximum amplitude (FDHM, ms), time to peak (TtP, ms), and Tau (ms). 2-APB abolished the sparks and thus parameters could not be measured in these conditions.

	Means ± S.E.				
	Amplitude	FWHM	FDHM	TtP	Tau
RGS4$^{+/+}$	0.76 ± 0.02	2.26 ± 0.04	34.08 ± 0.91	22.39 ± 1.82	38.59 ± 1.82
RGS4$^{-/-}$	0.62 ± 0.02	2.44 ± 0.13	46.27 ± 1.36	29.70 ± 1.26	70.11 ± 8.85
RGS4$^{+/+}$ with ET-1	0.61 ± 0.03	2.46 ± 0.08	36.68 ± 1.92	22.77 ± 1.57	42.18 ± 3.87
RGS4$^{-/-}$ with ET-1	0.50 ± 0.01	2.34 ± 0.04	33.21 ± 0.89	23.63 ± 1.07	37.67 ± 2.32

The Basic Properties of Calcium Handling in Murine Atria—We first characterized the basic properties of calcium sparks and transients in murine atrial myocytes. Sparks occurred spontaneously in murine atrial myocytes, although there was some variation between cells in number. They were likely mediated by calcium release via the ryanodine receptors because they were increased in frequency by caffeine and significantly decreased by tetracaine. In the case of caffeine, some of the events became longer and broader similar to waves. The IP_3 receptor inhibitor, 2-APB had variable effects on cells in the basal state with a net decrease on average (Fig. 4*A*). The sparks were located throughout the cell with some

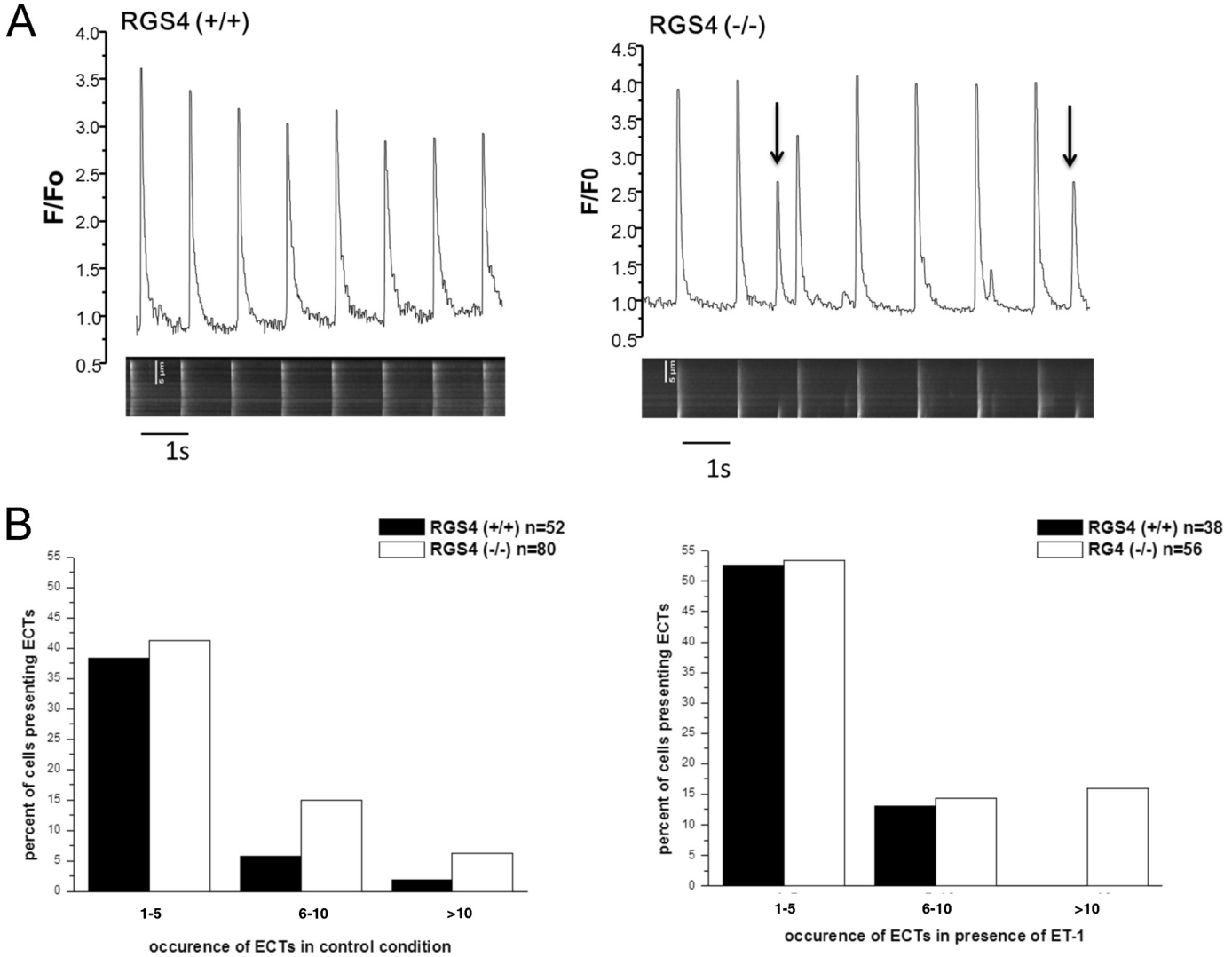

FIGURE 6. **RGS4 and the occurrence of ECTs.** *A*, representative traces showing the increased occurrence of ECTs (*arrows*) in the atrial cardiomyocytes from RGS4$^{+/+}$ and RGS4$^{-/-}$ mice in the absence of endothelin. *B*, the number of ECTs was greater in RGS4$^{-/-}$ mice. ET-1 (0.1 μM) increases the number of ETCs in both RGS4$^{+/+}$ and RGS4$^{-/-}$.

clustering toward the membrane (Fig. 4*B*). We saw a similar pattern with the calcium transient initiated by stimulation in atrial tissue sheets. Caffeine increased the transient size, and tetracaine largely abolished it. However, in these conditions 2-APB was without effect in the absence of receptor activation (Fig. 4*C*).

Increased Calcium Spark Frequency in RGS4$^{-/-}$ Mice—The alternative possibility is that RGS4 is acting as a GTPase-activating protein for the $G_{q/11}$ family of G-proteins. To address this hypothesis, we studied Ca^{2+} handling in single atrial cells by measuring elementary Ca^{2+} release events ("sparks") in the absence and presence of ET-1: an agonist at endothelin receptors that are predominantly coupled to $G_{q/11}$. The major difference was a significant increase in the frequency of Ca^{2+} release events in the RGS4$^{-/-}$ mice compared with RGS4$^{+/+}$ mice both in the absence (10.70 ± 2.17 *versus* 3.20 ± 0.74 sparks in 25 and 28 cells, respectively, $p < 0.001$) and presence (23.64 ± 4.26 *versus* 6.51 ± 1.05 sparks in 19 and 13 cells, respectively, $p < 0.01$) of ET-1 (Fig. 5, *A* and *B*). The cells were isolated from at least three independent mice in each genotype. 2-APB, an inhibitor of intracellular IP_3 receptors, completely abolished the sparks in both untreated and in ET-1-treated cells (Fig. 5*A*). In all cases, the sparks had the same spatial width but were slightly reduced in fluorescence amplitude in RGS4$^{-/-}$ cells in the absence of ET-1 (Table 4). However, the sparks were longer in duration. These differences disappeared upon the addition of ET-1 (Table 3).

Spontaneous Ca^{2+} Release Events in Field Stimulated Cells—We then moved on to examine global Ca^{2+} transients after field stimulating single atrial myocytes based on previous studies (24). The transients were larger in RGS4$^{-/-}$ cells compared with control cells: $F/F_0 = 3.34 \pm 0.16$ in RGS4$^{-/-}$ ($n = 54$), $F/F_0 = 2.66 \pm 0.14$ in RGS4 ($n = 40$), $p < 0.01$. There was no difference in the duration of the transients (446 ± 23 *versus* 483 ± 23, $p > 0.05$). Furthermore, in RGS4$^{-/-}$ cells, we noticed a significant increase in the number of ECTs that occurred during a pacing train in a line scan both in the absence and presence of ET-1 (Fig. 6). In RGS4$^{+/+}$, 44% (23 of 52) *versus* RGS4$^{-/-}$ 64% (51 of 80, $p = 0.03$ Fisher's exact test) had ECTs. In cells treated with ET-1:

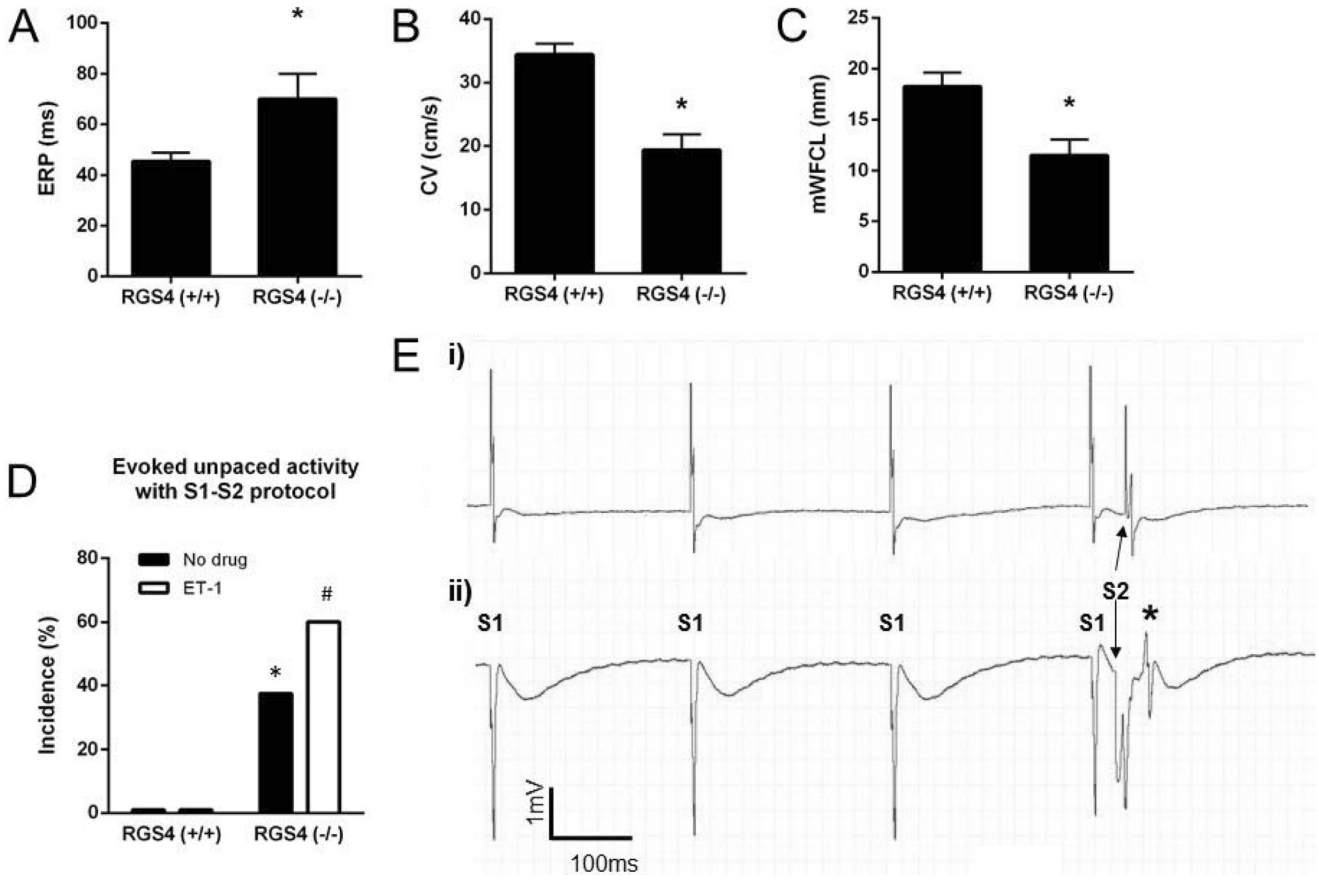

FIGURE 7. **The electrophysiology of isolated left atria.** *A*, atrial effective refractory period. *B* and *C*, conduction velocity (*B*) and minimum wave front cycle length (*C*, *mWFCL*) were all slightly altered in left atrial tissue deficient in RGS4$^{-/-}$ mice compared with RGS4$^{+/+}$ ($n = 13$ for RGS4$^{+/+}$ and $n = 8$ for RGS4$^{-/-}$; * p value <0.05 by t test). *D*, percentage of atria in which unpaced evoked activity was induced by S1-S2 protocol in absence or in presence of ET-1 in 13 RGS4$^{+/+}$ and 8 RGS4$^{-/-}$ mice. * and #, p value <0.05 by Fisher's exact test *versus* RGS4$^{+/+}$ mice in the absence and presence, respectively, of ET-1. *E*, representative traces of field potential recording during S1-S2 pacing protocol in RGS4$^{+/+}$ (*panel i*) and RGS4$^{-/-}$ (*panel ii*) atria in the presence of 10 nM ET-1, with the latter showing evoked abnormal activity (*).

RGS4$^{+/+}$ 66% (25 of 38) *versus* RGS4$^{-/-}$ 84% (47 of 56, $p = 0.05$ Fisher's exact test). We measured the distribution of the number of events in the pacing train. When they occurred, there were higher numbers of them in knock-out cells per line scan (Fig. 6*B*). We compared the frequency of ECTs (RGS4$^{+/+}$ *versus* RGS4$^{-/-}$ with and without ET-1) using two-way analysis of variance. The effect of both genotype ($p < 0.01$) and endothelin ($p < 0.001$) is significant.

Ex Vivo Tissue Electrophysiology—We performed an analysis of the tissue electrophysiology in isolated left atria using a multielectrode array. In RGS4$^{-/-}$ atria, there was a prolonged ERP and decreased conduction velocity in comparison to RGS4$^{+/+}$, resulting in a small decrease in potential path length for re-entry (Fig. 7, *A–C*). Using S1-S2 pacing trains, RGS4$^{+/+}$ atria did not display any unpaced electrical events, even after addition of ET-1 in the superfusion solution (Fig. 7, *D* and *E*). In contrast, RGS4$^{-/-}$ left atria developed abnormal unpaced events after pacing trains in both the absence and presence of ET-1 (Fig. 7, *D* and *E*).

Histological Studies—Histological studies revealed no structural abnormalities in atria or ventricles in five control and RGS4$^{-/-}$ mice, suggesting that the etiology was primarily electrophysiological (not shown).

Discussion

The unique findings are that the absence of RGS4 predisposes mice to abnormal calcium release events in atrial myocytes and inducible atrial fibrillation as previously reported (10). The mice are also tachycardic and have an increased bradycardic response to carbachol consistent with previous findings (9). There were no structural abnormalities, suggesting a primary electrophysiological etiology. Atrial cells from RGS4$^{-/-}$ mice show abnormal Ca^{2+} handling with increased Ca^{2+} spark frequency potentiated by activation of endothelin receptors and abnormal Ca^{2+} release and electrical events after a pacing train. The data are consistent with RGS4 being an important GTPase-activating protein for the $G_{q/11}$ pathway in atrial myocytes. The subsequent increased generation of IP_3 leads to a higher frequency of elemental Ca^{2+} events, abnormal Ca^{2+} release, and electrical events and a potential proarrhythmic substrate as discussed below.

Cardiac myocytes are thought to express a number of RGSs with a significant potential for redundancy in function (25–27). Parasympathetic control of heart rate in the SA node has been attributed to both RGS4 and RGS6 (9, 11, 12). Our studies were consistent with published studies and with an important role of RGS4 in the SA node in damping down the normal vagal input.

However, under resting conditions, the RGS4$^{-/-}$ mice were tachycardic, suggesting that RGS4 might have roles outside of the heart in regulating heart rate, for example, in central brainstem control centers (28). It is a possibility that the absence of RGS4 might be expected to increase GIRK channel currents in the atria, as well as the SA node, shortening the atrial effective refractory period and perhaps promoting atrial arrhythmia. In general, RGS4 is thought to be more highly expressed in the SA node than in the atria (12). We did not see any differences in the dynamics of GIRK activation and desensitization after muscarinic receptor activation in single atrial cells in contrast to the findings on cells isolated from the SA node. This assay is a sensitive method for determining the actions of RGS on inhibitory G-proteins (23). The only significant change was a modest increase in deactivation rate in the RGS4$^{-/-}$ mouse compared with littermate controls. This may be accounted for by compensatory increases in the expression of other RGSs or other indirect signaling effects related to the loss of RGS4. This would be consistent with the idea that other more highly expressed RGS (*e.g.* RGS6) that predominantly interact with inhibitory G-protein α subunits are able to compensate for the loss of RGS4.

RGS4 and Calcium Signaling in the Atria—The potential role of abnormal Ca^{2+} signaling in initiating atrial fibrillation is currently topical (29). Differences exist between atrial and ventricular cardiomyocytes in Ca^{2+} handling, and this affects susceptibility to arrhythmia. In general, there are fewer transverse tubules (and some species do not have them) present in atria compared with ventricles, and as a result more calcium release units are located beneath the plasmalemmal rather than t-tubular membrane (30). In addition, there is a more highly developed IP_3 receptor system in atria than in the ventricle (31). IP_3 in atrial cardiomyocytes causes spontaneous $[Ca^{2+}]_i$ transients, Ca^{2+} waves, and alternans, as well as early and delayed afterdepolarizations, which are all potentially proarrhythmic (32). These effects were abolished by the IP_3 receptor antagonist 2-APB and in IP_3 receptor 2 knock-out mice (33). Endothelin is a potent stimulus to initiate IP_3-related calcium events. This leads to spatially restricted Ca^{2+} release events and diastolic afterdepolarizations (24). Intriguingly, in this paper the authors presented evidence for colocalization of ryanodine and IP_3 receptors, with the latter sensitizing release (24). Our own data are very much consistent with this hypothesis.

RGS4 is able to act as a GTPase-activating protein for G-proteins of the $G_{q/11}$ family (14). Thus it is plausible that RGS4 deficiency in atrial myocytes promotes conditions in which there is greater IP_3-related Ca^{2+} release from intracellular stores, both under resting conditions and after activation of endothelin receptors, which predominantly couple to this family of G-protein, and this in turn is proarrhythmic. It is known that endothelin-1 levels are increased in patients with AF (34). The increased spark frequency and abnormal Ca^{2+} release and electrical events in single cells and intact left atria strongly supports this as the potential mechanism. Others have noted the predisposition to AF in RGS4 -deficient mice, although there was little study of the potential mechanism7 and we made the basic observation earlier (published in abstract form) (10, 35). The implication was made (although not tested) that down-regulation RGS4 during endurance training in rats was responsible for increased GIRK channel activity and predisposition to AF (10). RGS2 deficiency, which also acts as a GTPase-activating protein for $G_{q/11,}$ has also been associated with AF, although the mechanism was not clearly related to Ca^{2+} handling (36).

Spontaneous AF was not found in our study but could be consistently induced by atrial burst pacing. The duration of AF was not significantly different between RGS4$^{+/+}$ and RGS4$^{-/-}$ mice, and this suggests we may be looking at a factor that is important for initiating rather than sustaining AF. For the most part, AF was not prolonged in duration, suggesting that the AF rotor eventually dies out, and this effect may be related to the small size of atrial tissue in the mouse. The nonsustained nature of AF may explain why spontaneous or permanent episodes are not seen because any short paroxysms do not allow sufficient time for electrophysiological and structural remodeling (7). Programmed electrical stimulation was less consistent in our hands in provoking AF even after the administration of carbachol. It is also clear that burst pacing promotes Ca^{2+} accumulation within the paced myocardium. Thus enhanced intracellular Ca^{2+} release will lead to enhanced inward Na^+-Ca^{2+} exchange current and to diastolic afterdepolarizations (17, 29). We saw direct evidence that such was occurring in field-stimulated single atrial myocytes (Fig. 6) and in isolated whole left atria studied using a microelectrode array (Fig. 7).

We also noted an increase in the action potential duration in single cells and in the atrial effective refractory period in intact whole left atria. This was combined with a decrease in conduction velocity. The net effect of this was to modestly reduce the wavefront cycle length, which could also be proarrhythmic (see the discussion above, however). The increased intracellular calcium flux may increase inward current through the sodium-calcium exchanger, which would prolong the action potential duration and lead to a modest lengthening of the ERP. We did try benzamil, but this rendered the tissue slices no longer excitable. It is also known that increases in intracellular Ca^{2+} and PKC phosphorylation can promote a decrease in gap junction function (37, 38). Finally, there may be some differences in autonomic balance *in vivo*, which would not be recapitulated *ex vivo* in the slices and cells.

In summary, we have identified RGS4 deficiency as a factor in the initiation of AF. Our results also highlight the potential therapeutic importance of modulating the $G_{q/11}$-IP_3-Ca^{2+} signaling axis. Direct activation of RGS4 or increasing protein levels by interfering with its degradation could inhibit episodes of AF (39), and conversely inhibition of RGS action may have proarrhythmic effects.

Author Contributions—A. O., M. N., D. M., R. B., and A. T. designed the research; A. O., M. N., D. M., N. A., M. F., and R. B. performed the research; and A. O., M. N., D. M., M. F., R. B., and A. T. analyzed the data and wrote the paper.

References

1. Benjamin, E. J., Wolf, P. A., D'Agostino, R. B., Silbershatz, H., Kannel, W. B., and Levy, D. (1998) Impact of atrial fibrillation on the risk of death: the Framingham Heart Study. *Circulation* **98,** 946–952
2. Nattel, S. (2002) New ideas about atrial fibrillation 50 years on. *Nature*

415, 219–226
3. Beaumont, J., Davidenko, N., Davidenko, J. M., and Jalife, J. (1998) Spiral waves in two-dimensional models of ventricular muscle: formation of a stationary core. *Biophys. J.* **75,** 1–14
4. Pandit, S. V., and Jalife, J. (2013) Rotors and the dynamics of cardiac fibrillation. *Circ. Res.* **112,** 849–862
5. Haïssaguerre, M., Jaïs, P., Shah, D. C., Takahashi, A., Hocini, M., Quiniou, G., Garrigue, S., Le Mouroux, A., Le Métayer, P., and Clémenty, J. (1998) Spontaneous initiation of atrial fibrillation by ectopic beats originating in the pulmonary veins. *N. Engl. J. Med.* **339,** 659–666
6. Wijffels, M. C., Kirchhof, C. J., Dorland, R., and Allessie, M. A. (1995) Atrial fibrillation begets atrial fibrillation. A study in awake chronically instrumented goats. *Circulation* **92,** 1954–1968
7. Allessie, M., Ausma, J., and Schotten, U. (2002) Electrical, contractile and structural remodeling during atrial fibrillation. *Cardiovasc. Res.* **54,** 230–246
8. Tinker, A. (2006) The selective interactions and functions of regulators of G-protein signalling. *Semin. Cell Dev. Biol.* **17,** 377–382
9. Cifelli, C., Rose, R. A., Zhang, H., Voigtlaender-Bolz, J., Bolz, S. S., Backx, P. H., and Heximer, S. P. (2008) RGS4 regulates parasympathetic signaling and heart rate control in the sinoatrial node. *Circ. Res.* **103,** 527–535
10. Guasch, E., Benito, B., Qi, X., Cifelli, C., Naud, P., Shi, Y., Mighiu, A., Tardif, J. C., Tadevosyan, A., Chen, Y., Gillis, M. A., Iwasaki, Y. K., Dobrev, D., Mont, L., Heximer, S., and Nattel, S. (2013) Atrial fibrillation promotion by endurance exercise: demonstration and mechanistic exploration in an animal model. *J. Am. Coll. Cardiol.* **62,** 68–77
11. Yang, J., Huang, J., Maity, B., Gao, Z., Lorca, R. A., Gudmundsson, H., Li, J., Stewart, A., Swaminathan, P. D., Ibeawuchi, S. R., Shepherd, A., Chen, C. K., Kutschke, W., Mohler, P. J., Mohapatra, D. P., Anderson, M. E., and Fisher, R. A. (2010) RGS6, a modulator of parasympathetic activation in heart. *Circ. Res.* **107,** 1345–1349
12. Posokhova, E., Wydeven, N., Allen, K. L., Wickman, K., and Martemyanov, K. A. (2010) RGS6/Gss5 complex accelerates IKACh gating kinetics in atrial myocytes and modulates parasympathetic regulation of heart rate. *Circ. Res.* **107,** 1350–1354
13. Posokhova, E., Ng, D., Opel, A., Masuho, I., Tinker, A., Biesecker, L. G., Wickman, K., and Martemyanov, K. A. (2013) Essential role of the m2R-RGS6-IKACh pathway in controlling intrinsic heart rate variability. *PLoS One* **8,** e76973
14. Hepler, J. R., Berman, D. M., Gilman, A. G., and Kozasa, T. (1997) RGS4 and GAIP are GTPase-activating proteins for Gqα and block activation of phospholipase Cβ by γ-thio-GTP-Gqα. *Proc. Natl. Acad. Sci. U.S.A.* **94,** 428–432
15. Ross, E. M., and Wilkie, T. M. (2000) GTPase-activating proteins for heterotrimeric G proteins: regulators of G protein signaling (RGS) and RGS-like proteins. *Annu. Rev. Biochem.* **69,** 795–827
16. Wieland, T., Lutz, S., and Chidiac, P. (2007) Regulators of G protein signalling: a spotlight on emerging functions in the cardiovascular system. *Curr. Opin. Pharmacol.* **7,** 201–207
17. Janvier, N. C., McMorn, S. O., Harrison, S. M., Taggart, P., and Boyett, M. R. (1997) The role of Na^+-Ca^{2+} exchange current in electrical restitution in ferret ventricular cells. *J. Physiol* **504,** 301–314
18. Zuberi, Z., Nobles, M., Sebastian, S., Dyson, A., Lim, S. Y., Breckenridge, R., Birnbaumer, L., and Tinker, A. (2010) Absence of the inhibitory G-protein, $G\alpha_{i2}$, predisposes to ventricular cardiac arrhythmia. *Circ. Arrhythm. Electrophysiol.* **3,** 391–400
19. Picht, E., Zima, A. V., Blatter, L. A., and Bers, D. M. (2007) SparkMaster: automated calcium spark analysis with ImageJ. *Am. J. Physiol. Cell Physiol.* **293,** C1073–C1081
20. Bussek, A., Schmidt, M., Bauriedl, J., Ravens, U., Wettwer, E., and Lohmann, H. (2012) Cardiac tissue slices with prolonged survival for *in vitro* drug safety screening. *J. Pharmacol. Toxicol. Methods* **66,** 145–151
21. Thomas, S. A., Schuessler, R. B., Berul, C. I., Beardslee, M. A., Beyer, E. C., Mendelsohn, M. E., and Saffitz, J. E. (1998) Disparate effects of deficient expression of connexin43 on atrial and ventricular conduction: evidence for chamber-specific molecular determinants of conduction. *Circulation* **97,** 686–691
22. Benians, A., Nobles, M., Hosny, S., and Tinker, A. (2005) Regulators of G-protein signalling form a quaternary complex with the agonist, receptor and G-protein: a novel explanation for the acceleration of signalling activation kinetics. *J. Biol. Chem.* **280,** 13383–13394
23. Benians, A., Leaney, J. L., and Tinker, A. (2003) Agonist unbinding from receptor dictates the nature of deactivation kinetics of G-protein gated K^+ channels. *Proc. Natl. Acad. Sci. U.S.A.* **100,** 6239–6244
24. Mackenzie, L., Bootman, M. D., Laine, M., Berridge, M. J., Thuring, J., Holmes, A., Li, W. H., and Lipp, P. (2002) The role of inositol 1,4,5-trisphosphate receptors in Ca(2+) signalling and the generation of arrhythmias in rat atrial myocytes. *J. Physiol* **541,** 395–409
25. Doupnik, C. A., Xu, T., and Shinaman, J. M. (2001) Profile of RGS expression in single rat atrial myocytes. *Biochim. Biophys. Acta* **1522,** 97–107
26. Owen, V. J., Burton, P. B., Mullen, A. J., Birks, E. J., Barton, P., and Yacoub, M. H. (2001) Expression of RGS3, RGS4 and Giα2 in acutely failing donor hearts and end-stage. *Eur. Heart J.* **22,** 1015–1020
27. Mittmann, C., Chung, C. H., Höppner, G., Michalek, C., Nose, M., Schüler, C., Schuh, A., Eschenhagen, T., Weil, J., Pieske, B., Hirt, S., and Wieland, T. (2002) Expression of ten RGS proteins in human myocardium: functional characterization of an upregulation of RGS4 in heart failure. *Cardiovasc. Res.* **55,** 778–786
28. Spyer, K. M. (1994) Annual review prize lecture. Central nervous mechanisms contributing to cardiovascular control. *J. Physiol* **474,** 1–19
29. Voigt, N., Li, N., Wang, Q., Wang, W., Trafford, A. W., Abu-Taha, I., Sun, Q., Wieland, T., Ravens, U., Nattel, S., Wehrens, X. H., and Dobrev, D. (2012) Enhanced sarcoplasmic reticulum Ca^{2+} leak and increased Na^+-Ca^{2+} exchanger function underlie delayed afterdepolarizations in patients with chronic atrial fibrillation. *Circulation* **125,** 2059–2070
30. Sheehan, K. A., and Blatter, L. A. (2003) Regulation of junctional and non-junctional sarcoplasmic reticulum calcium release in excitation-contraction coupling in cat atrial myocytes. *J. Physiol.* **546,** 119–135
31. Kockskämper, J., Zima, A. V., Roderick, H. L., Pieske, B., Blatter, L. A., and Bootman, M. D. (2008) Emerging roles of inositol 1,4,5-trisphosphate signaling in cardiac myocytes. *J. Mol. Cell Cardiol.* **45,** 128–147
32. Kockskämper, J., and Blatter, L. A. (2002) Subcellular Ca^{2+} alternans represents a novel mechanism for the generation of arrhythmogenic Ca^{2+} waves in cat atrial myocytes. *J. Physiol.* **545,** 65–79
33. Li, X., Zima, A. V., Sheikh, F., Blatter, L. A., and Chen, J. (2005) Endothelin-1-induced arrhythmogenic Ca^{2+} signaling is abolished in atrial myocytes of inositol-1,4,5-trisphosphate (IP3)-receptor type 2-deficient mice. *Circ. Res.* **96,** 1274–1281
34. Mayyas, F., Niebauer, M., Zurick, A., Barnard, J., Gillinov, A. M., Chung, M. K., and Van Wagoner, D. R. (2010) Association of left atrial endothelin-1 with atrial rhythm, size, and fibrosis in patients with structural heart disease. *Circ. Arrhythm. Electrophysiol.* **3,** 369–379
35. Opel, A., and Tinker, A. (2011) RGS 4 KO mice are pre-disposed to atrial fibrillation and show disrupted sympathovagal balance *in vivo*, making RGS 4 a potential novel therapeutic target for atrial fibrillation. *Europace* **13,** vi 17
36. Tuomi, J. M., Chidiac, P., and Jones, D. L. (2010) Evidence for enhanced M3 muscarinic receptor function and sensitivity to atrial arrhythmia in the RGS2-deficient mouse. *Am. J. Physiol. Heart Circ. Physiol.* **298,** H554–H561
37. De Groot, J. R., and Coronel, R. (2004) Acute ischemia-induced gap junctional uncoupling and arrhythmogenesis. *Cardiovasc. Res.* **62,** 323–334
38. Márquez-Rosado, L., Solan, J. L., Dunn, C. A., Norris, R. P., and Lampe, P. D. (2012) Connexin43 phosphorylation in brain, cardiac, endothelial and epithelial tissues. *Biochim. Biophys. Acta* **1818,** 1985–1992
39. Davydov, I. V., and Varshavsky, A. (2000) RGS4 is arginylated and degraded by the N-end rule pathway *in vitro*. *J. Biol. Chem.* **275,** 22931–22941